A method to determine composite material residual tensile strength in the fibre direction as a function of the matrix damage state after fatigue loading

Damien Caous [a, b, *], Christophe Bois [c], Jean-Christophe Wahl [c], Thierry Palin-Luc [b], Julien Valette [a, c]

[a] TENSYL, 48 Rue Jacques de Vaucanson, Pôle Arts&Métiers, 17180 Périgny, France
[b] Arts et Métiers ParisTech, I2M, CNRS, Esplanade des Arts et Métiers, 33405 Talence, France
[c] Université de Bordeaux, I2M, CNRS, 15 Rue Naudet, 33170 Gradignan, France

A B S T R A C T

The phenomenon of residual strength in composite laminates after fatigue loading has been studied for decades but is generally expressed as a function of the number of cycles applied to the specimens. Phenomenological laws deduced from these tests are therefore loading dependent and identifying a valid model for any loading condition of a given laminate requires long fatigue testing campaigns. To overcome this difficulty, a testing procedure is proposed to express the residual tensile strength of a unidirectional ply in the fibre direction, as a function of its matrix damage. The resulting behaviour is then independent of the imposed loading and can be determined by only a few fatigue tests. Experimental results obtained on glass-epoxy non-crimp fabric laminates are presented and analysed.

Keywords:
Lamina/ply
Fatigue
Strength
Damage mechanics

1. Introduction

Composite laminates with unidirectional (UD) plies have been studied for several decades and damage modes, either under monotonic quasi-static or fatigue loadings, have been well identified [1–11]. It has been shown that fibre-matrix decohesions or matrix microcracks lead to intralaminar cracks which propagate until they reach a ply interface, where they can result in delamination (Fig. 1).

All these damage mechanisms induce several phenomena at the ply scale which have consequences for ply and laminate behaviour, depending on the loading direction. Under transverse or shear loading, UD ply behaviour is non-linear and can be expressed as a loss of stiffness - commonly called residual stiffness - and a residual strain. These phenomena are observed either under monotonic quasi-static [12–14] or fatigue loadings [15–17] for transverse and shear behaviour. They are due to the same damage mechanisms (fibre-matrix decohesion and matrix cracking), which leads to strong coupling between shear and transverse damage [18,19].

Under loading in the fibre direction, UD plies have a linear elastic brittle behaviour and neither residual stiffness nor residual strain is observed. However, under fatigue loading, a residual strength phenomenon is observed which reflects the fact that if fatigue load is high enough, the static load that the material could sustain will be less than the load it was able to sustain before fatigue loading [20–22] (Fig. 2). This phenomenon is explained by the fact that once a matrix is damaged by fibre-matrix decohesion and matrix cracks, it progressively loses its capacity to transfer loads between all the fibres of the ply. As soon as loads cannot be distributed to all fibres of the ply, deviations in material configuration will make some fibres more loaded than others and early progressive fibre failures in the ply will result in a decrease in its strength [23].

Studying residual strength and stiffness is not only advantageous when describing composite laminate behaviour under fatigue loading, but when both are combined, it is possible to assess the fatigue life of any laminate from UD ply data [23–26] (Fig. 3).

Damage mechanisms under a specific stress state in each ply under fatigue loading will lead to stiffness and strength degradations. Stiffness degradation will have an impact on stress

* Corresponding author. TENSYL, 48 rue Jacques de Vaucanson, Pôle Arts&Métiers, 17180 Périgny, France.
E-mail address: damien.caous@tensyl.com (D. Caous).

Nomenclature

NCF	non-crimp fabric
UD	unidirectional
x-axis	laminate loading direction
y-axis	axis perpendicular to *x-axis* within the laminate plane
1-axis	ply fibre direction
2-axis	ply transverse direction
D	fibre diameter
d_{12}	damage parameter: residual shear stiffness
d_m	fitting parameter
d_λ	fitting parameter
F_x	axial force
G_{12}^0	initial shear modulus of the UD ply
G_{12}	damaged shear modulus of the UD ply
L	long axis of an ellipse
S	specimen section
ε_x	strain of the laminate in the loading direction
ε_y	strain of the laminate in *y-axis* direction
γ_{12}	total shear strain in the ply coordinate system
θ	ply angle
σ_0	residual tensile strength of the UD ply, in the fibre direction, before matrix damage
σ_T	residual tensile strength of the UD ply, in the fibre direction, at glass transition temperature
σ_x	axial stress at the laminate scale
τ_{12}	shear stress in the ply coordinate system
$\|x\|$	absolute value of x

distribution at both laminate and structure scales. Consequently, fatigue failure will occur when the maximum stress in the material meets the residual strength. Iterative calculations, including progressive stiffness degradation at the ply scale, are therefore relevant for computing the fatigue life of any stacking sequence.

The most common way to study residual strength is to express it as a function of the number of cycles applied to the material in a particular loading condition. Several comprehensive reviews and comparisons of such phenomenological approaches are available in the literature [27–30]. All of them draw the same conclusions: such models have the drawback that they are valid only for the loading condition used to identify them. Consequently, large testing campaigns are needed to identify a law valid for all the loading conditions, including multiaxial stress states. As stress states in UD plies are strongly multiaxial, due to the lamination effect or external multiaxial loading [31], the difficulty of identifying residual strength has to be overcome.

Contrary to phenomenological approaches, damage mechanics approaches look at understanding damage mechanisms to assess the fatigue life of composite laminates. Since it has been shown that matrix damage (such as matrix cracks or fibre-matrix decohesion) penalizes load transfer between fibres and decreases the strength in the fibre direction, one solution, in the framework of damage mechanics approaches, is to express the residual strength in the fibre direction as a function of matrix damage that is responsible for strength decrease and depends on loading conditions. This is the approach proposed by ONERA [32] or LMA-Marseille [23], where the residual strength is expressed as a function of shear residual stiffness at the scale of the UD plies. These approaches have the

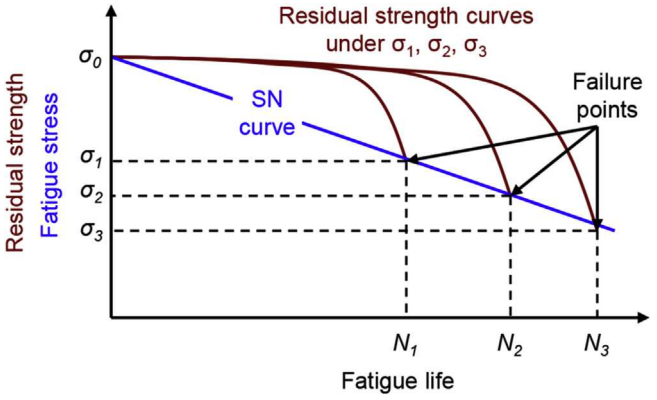

Fig. 2. Strength degradation of a laminate under constant uniaxial fatigue loading (according to [20–22]).

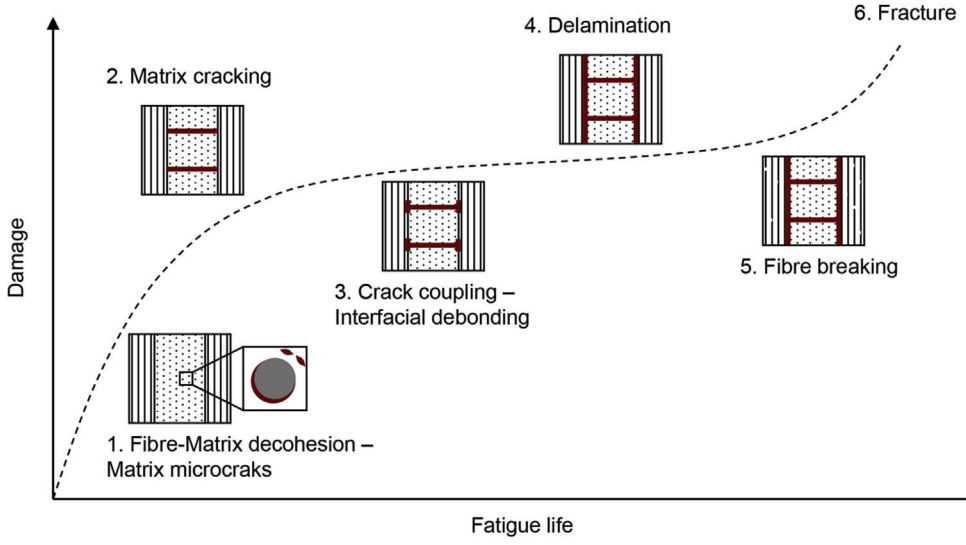

Fig. 1. Damage mechanisms in composite laminate under cyclic loading (according to [1] and [3]).

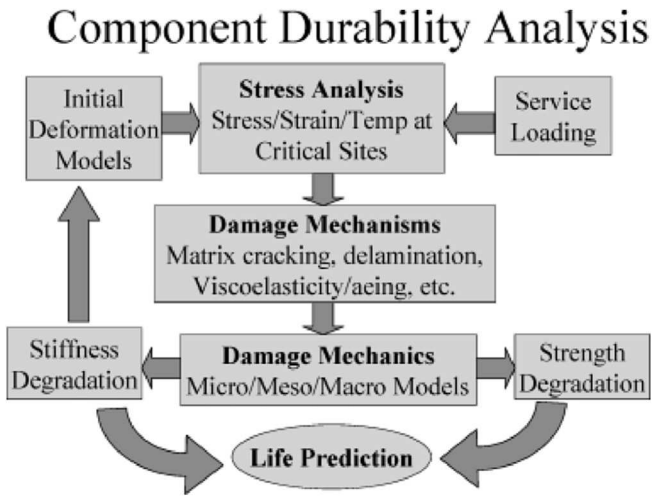

Fig. 3. Damage mechanics for component durability analysis [26].

double advantage, in theory, of computing the fatigue life of all laminate sequences under extended loading condition with a small testing campaign. This is due to the fact that residual strength is identified at the ply scale and expressed versus a damage parameter resulting from the entire ply loading history, including stress multi-axiality, monotonic load and the number of load cycles.

The work presented in this paper is part of a larger study on improving the fatigue life assessment of composite laminates for wind turbine blade applications. Due to very large blade dimensions and the low cost imposed in order to make power production profitable, the most frequently used manufacturing process for wind turbine blades is vacuum assisted resin infusion. Composite laminates are generally composed of non-crimp fabric (NCF) glass fibre or mixed glass-carbon reinforcements with thermoset resins like epoxy or polyester [33–36] (Fig. 4). The purpose of this study is to identify the dependency of the residual tensile strength of UD plies on the matrix damage, quantified as a decrease in shear stiffness. The novelty of the work presented here, with respect to the literature, is the proposal of a testing method to investigate the dependency previously described for plate specimens, which are representative of the material state in a wind turbine blade.

First, the material and experimental method are detailed, with a focus on the evaluation of matrix damage level according to the mechanical response. Then the results are presented and discussed before the conclusion and describe some proposals for future studies.

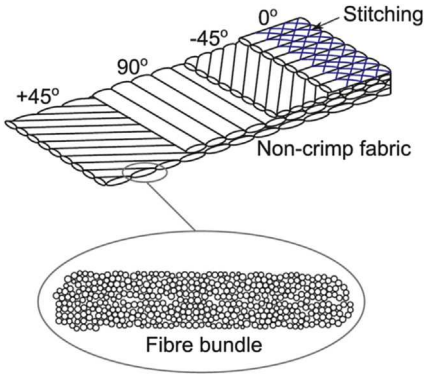

Fig. 4. Non-crimp fabric material [45].

2. Material and method

2.1. Composite material of the study

In this article, we consider 600 g/m^2 $[\pm 45]_{2s}$ NCF glass reinforcements with an epoxy resin system, as used in the wind turbine blade industry and manufactured by infusion. In the glass NCF reinforcement used here, ±45° UD plies are stitched together with a polyester yarn in order to make processing easier. The stitching pattern is known to have an influence on both damage growth and fatigue life [37]. However, by considering the same stitching pattern for all our tests, the residual strength results can be compared.

2.2. Test principle

The purpose of the testing procedure is to express the residual tensile strength of UD plies under monotonic quasi-static tensile loading along the fibre direction as a function of the matrix damage. Manufacturing tubes by infusion is a delicate operation which makes the experimental method based on a tension torsion test, as proposed by Hochard et al. [23], irrelevant. Therefore the methodology adopted here is based on plate specimen testing. Plates are easier to manufacture and are more representative of the material state of the industrial structure.

A large $[\pm 45]_{2s}$ composite laminate coupon is loaded under uniaxial fatigue in order to generate matrix damage by shear stress at the UD ply scale. Fatigue testing is stopped before reaching failure (Fig. 5a). Once the fatigue test is over, $[0/90]_{2s}$ coupons are extracted from the large fatigue damaged $[\pm 45]_{2s}$ coupons – by cutting at 45° to the axis of fatigue loading (Fig. 5b)– and loaded under monotonic quasi-static tension to determine the residual strength (Fig. 5c). Once the level of matrix damage is expressed in the form of a stiffness loss variable, the residual tensile strength of the $[0/90]_{2s}$ laminate, and then the residual tensile strength of the 0° plies can be expressed as a function of this matrix damage variable.

The coordinate systems used in this paper for ply and laminate are illustrated in Fig. 5: coordinate system (*1,2*) is linked to the UD ply with axis *1* in the fibre direction and axis *2* in the in-plane transverse direction. Coordinate system (*x,y*) is linked to the specimen where *x*-axis is the longitudinal axis in coincidence with the loading direction and *y*-axis is in the width of the specimen.

The following section details the method used to compute the damage variable which represents the matrix damage state generated by the cyclic loading.

2.3. Evaluation of matrix fatigue damage in $[\pm 45]_{2s}$ laminates

The laminate sequence [±45] was chosen for two reasons: first, it allows a quasipure shear loading in UD plies and second, shear stiffness loss due to damage in UD plies is easy to measure at the laminate scale.

Using the classical laminate theory [38] one can easily demonstrate that for a symmetric and balanced [±45] laminate loaded in the x-direction, the shear stain γ_{12} at the ply scale in the ply coordinate system can be computed from the longitudinal and transversal strains ε_x and ε_y measured on the laminate surface:

$$\gamma_{12} = \pm(\varepsilon_x - \varepsilon_y) \tag{1}$$

In the same way, the shear stress τ_{12} in each ply can be computed measuring longitudinal load applied to the laminate:

$$\tau_{12} = \pm\frac{1}{2}\sigma_x \tag{2}$$

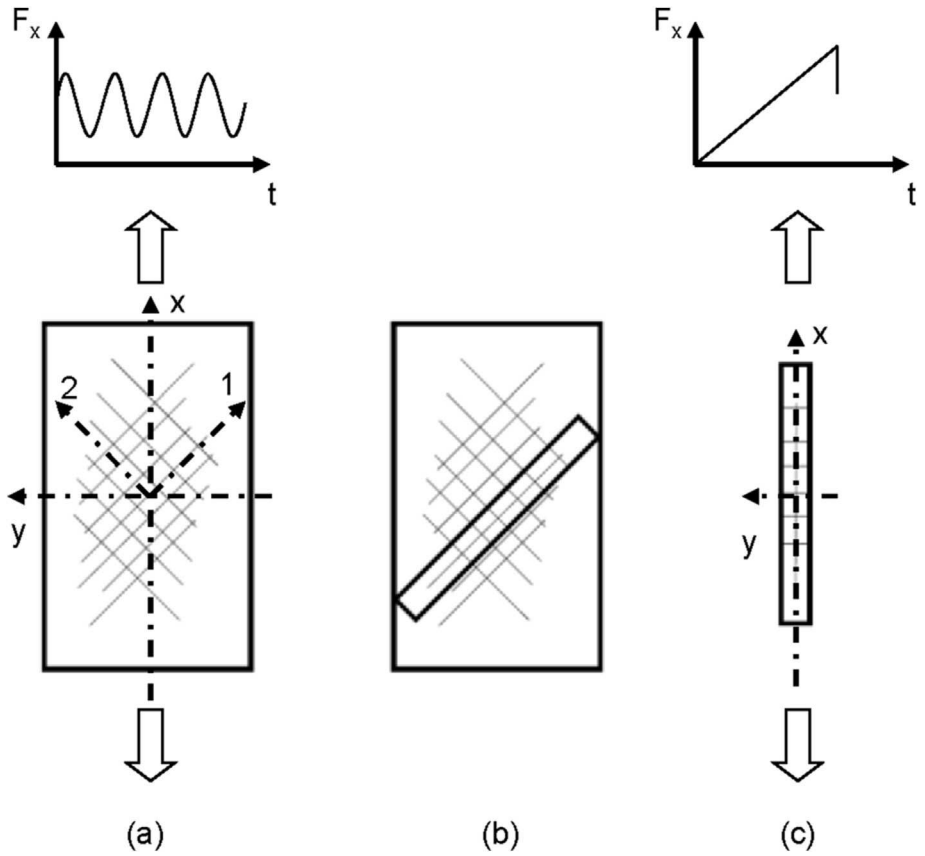

Fig. 5. Test principle: (a) Fatigue damage in $[\pm 45]_{2s}$ laminate (shear loading at the UD ply scale) (b) Extraction of $[0/90]_{2s}$ coupons from damaged $[\pm 45]_{2s}$ laminates (c) Residual tensile strength of 0° plies in $[0/90]_{2s}$ laminate.

with:

$$\sigma_x = \frac{F_x}{S} \tag{3}$$

where F_x is the load applied to the specimen and S is the area of the specimen cross section.

When a $[\pm 45]_{2s}$ laminate is loaded under static or fatigue, one can observe three kinds of damage consequences for its mechanical behaviour at the ply scale: residual strain, a hysteresis loop during the load-unload cycle and a decrease in secant stiffness. These three effects are generated both by the viscous behaviour of the polymer matrix (dissipative but reversible phenomenon), the sliding of existing damage (dissipative but reversible phenomenon) and damage growth (dissipative and irreversible phenomenon) [14,39]. Since these effects are strongly coupled, the definition of a proper damage variable to measure the matrix damage level is a key but non-obvious issue. Traditionally, the damage variable is defined as the secant stiffness loss measured on a load-unload cycle:

$$d_{12} = 1 - \frac{G_{12}}{G_{12}^0} \tag{4}$$

where G_{12} and G_{12}^0 are respectively the secant shear modulus associated with a certain level of damage and the initial shear modulus of the UD ply (Fig. 6a). However, this measurement is strongly dependent on both the load rate and the load level. In order to remove the load rate effect, we propose to measure the secant stiffness loss on low rate loading cycles performed before and after fatigue tests. In addition, reversible viscous residual strain is accumulated during fatigue loading. This residual strain, which decreases after unloading, can also produce an incorrect secant stiffness evaluation. The loading cycles used to measure the secant stiffness loss have therefore to be preceded by a relaxation step. It is worth noting that this method is consistent with damage measurement used for static analysis and modelling proposed in many studies [12, 15, 23].

The test procedure is summed up in Fig. 6 b. The loading rate used for the secant stiffness evaluation (20 MPa/min) and the duration of the relaxation step (1 h) was established with the help of preliminary tests. Note in Fig. 6 b that fatigue loops show an apparent stiffness that is higher than quasi-static loading due to the load rate effect and positive minimum fatigue stress. Note also that final stiffness is measured under quasi-static loading between zero stress up to the maximum stress applied during fatigue loading in order to take into account the load level effect.

As seen before, the measurement of the matrix damage variable, d_{12}, relies on the measurement of the axial force F_x, the axial strain ε_x and transversal strain ε_y of the laminate. However, a large width is necessary to extract specimens at 45° - from the axial loading - after fatigue testing, which means that the large $[\pm 45]_{2s}$ coupon is not slender enough to guarantee a homogeneous strain and stress field. A comparison of strain fields resulting from a numerical analysis between a standard slender specimen (250 mm × 25 mm) and the large specimen considered is illustrated in Fig. 7 at the ply scale. Geometry of the large $[\pm 45]_{2s}$ specimen is provided in Fig. 8 a. Both coupons were modeled by the finite element method and analysis was carried out with NASTRAN software, assuming material linear elastic behaviour and small perturbations. Four-node linear shell laminate elements are used so that the laminate can

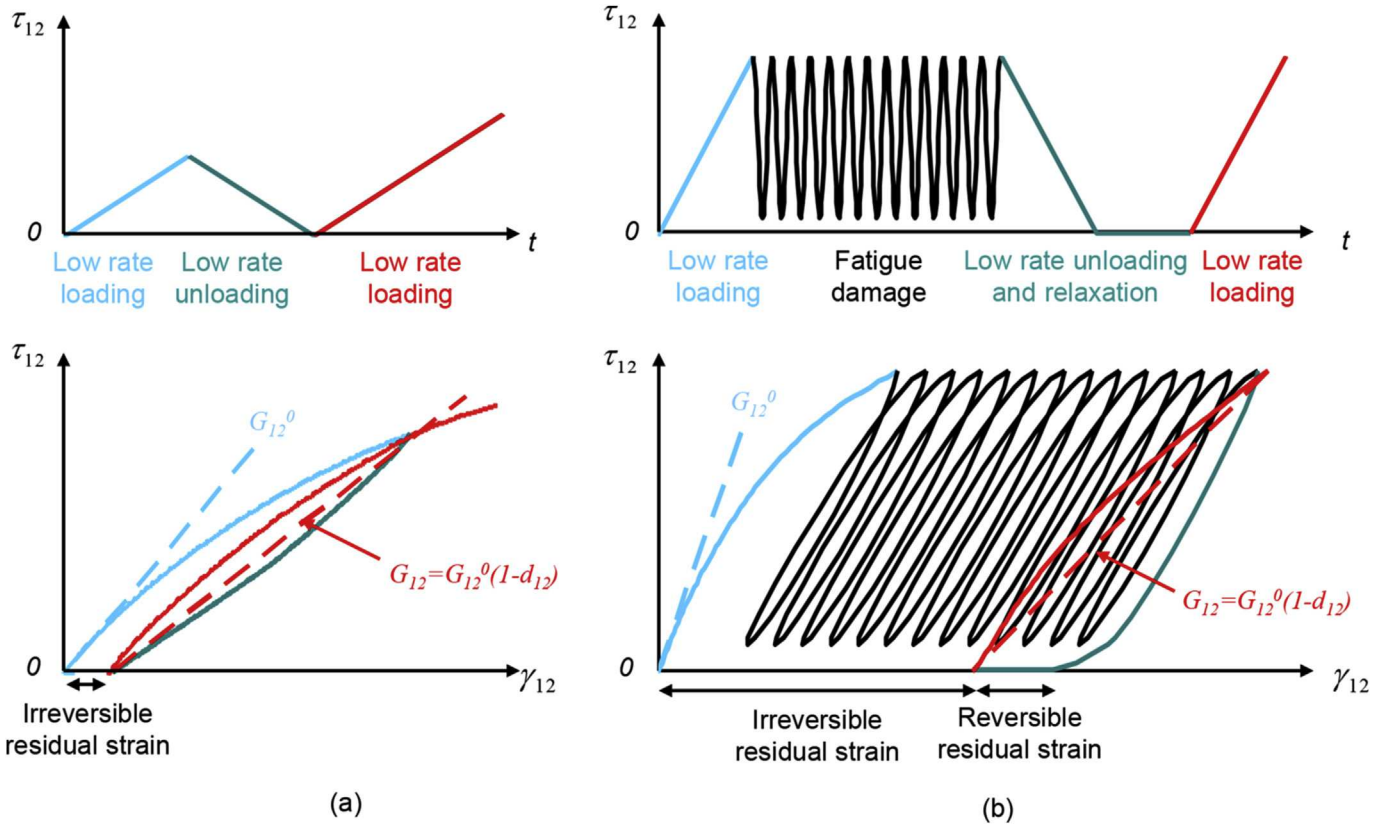

Fig. 6. (a) Definition of shear damage measurement in a $[\pm 45]_{2s}$ laminate under quasi-static loading (b) Shear damage generation and measurement procedure in a $[\pm 45]_{2s}$ laminate in tension-tension fatigue (R ~ 0.1).

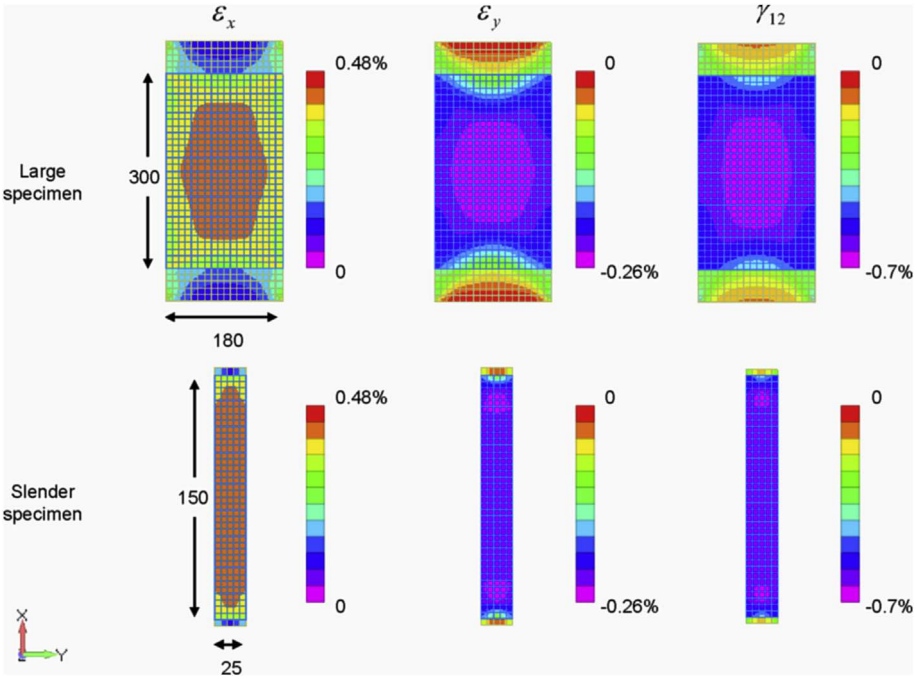

Fig. 7. Comparison of large and slender coupons: numerical strain fields in −45° UD ply.

be modelled UD ply by UD ply, and stresses and strains can be computed in each ply according to the classical laminate theory. Tab bonding is considered perfect and adhesive thickness is not taken into account. The degrees of freedom of the nodes at the grips are all blocked for one side of the specimen and all blocked on the other side, apart from translation in the longitudinal direction. A load is

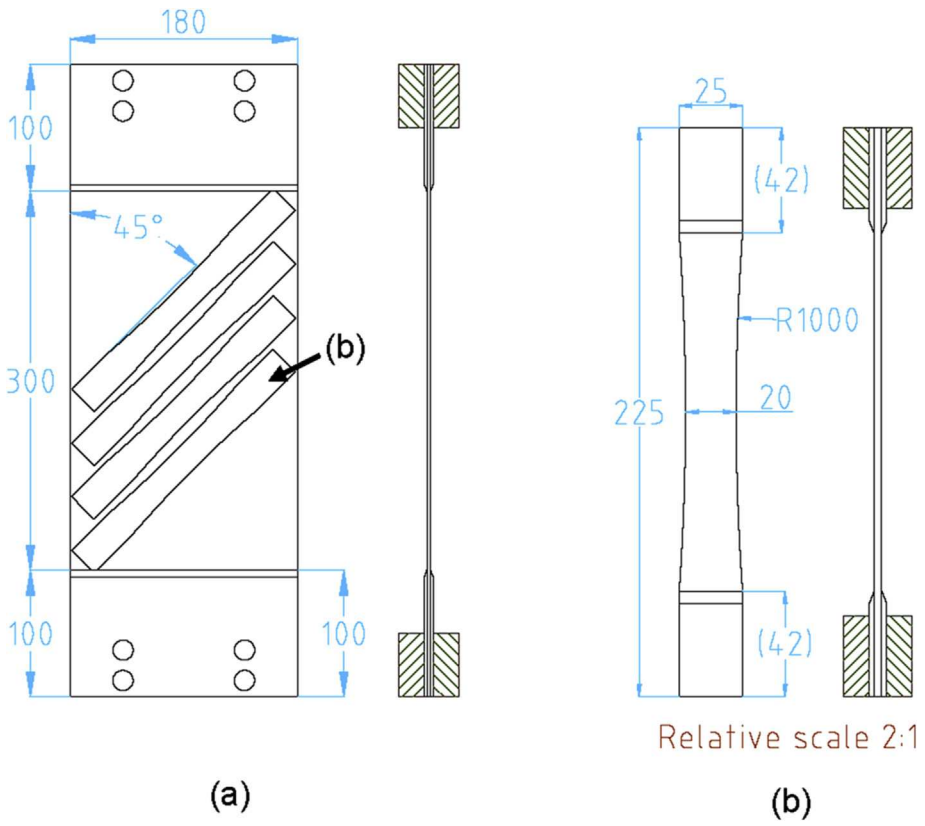

Fig. 8. (a) Large $[\pm 45]_{2s}$ specimen geometry for shear damage generation under fatigue loading (b) $[0/90]_{2s}$ extracted specimen geometry for residual tensile strength testing.

applied proportionally to the coupon section in order to generate the same theoretical nominal stress in each configuration. For the model of the slender specimen, one element of tab is kept outside the grips and for the large specimen model five elements of tab are kept outside the grips in order to model distance between grip end and tab end. Chamfers of tab are not accounted for.

Comparison of shear strain shows an inhomogeneous field in the large specimens. However, a quasi-homogeneous area can be used to extract four specimens and measure residual tensile strength (Fig. 7 and Fig. 8a).

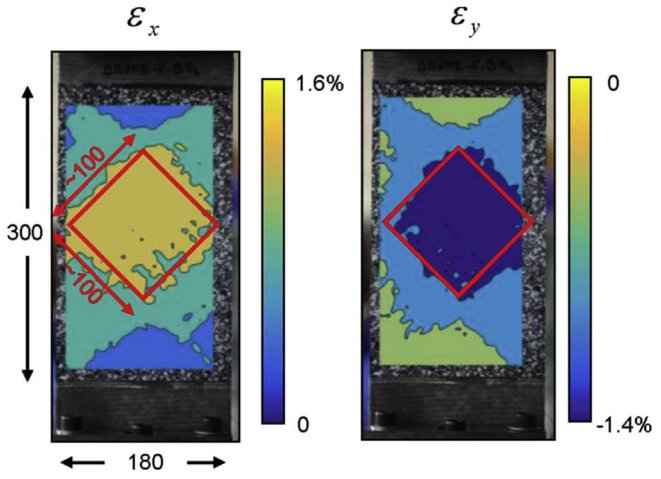

Fig. 9. Longitudinal and transversal strain field measured by digital image correlation on large $[\pm 45]_{2s}$ coupons after fatigue damage.

For d_{12} evaluation, shear strain γ_{12} is obtained by measuring the mean values of ε_x and ε_y by digital image correlation in a diamond-shaped area corresponding to the gauge area of the specimen dedicated to residual tensile strength tests (Fig. 9). In addition to strain variations as a result of the specimen geometry, which has been simulated (Fig. 7), a strain field heterogeneity and asymmetry near the tabs is observed (Fig. 9). In fact, material heterogeneity, small specimen misalignment and torsional degree of freedom of the upper grip can lead to errors in strain quantification. However, we specify that transverse strain is low near the tabs, which increase the impression of asymmetry.

Nevertheless, in the diamond-shaped area where d_{12} is evaluated, the relative standard deviation on strain is below 10%. Standard deviations obtained on the results detailed in section 3 show that damage is homogeneous enough in the extraction area to obtain relevant residual strength measurements.

Fatigue tests are performed with a 50 kN MTS hydraulic testing machine and digital image correlation is achieved with GOM-Aramis v6.3.0 system.

2.4. Residual tensile strength of $[0/90]_{2s}$ specimens

After fatigue testing on $[\pm 45]_{2s}$ plates, four $[0/90]_{2s}$ specimens are extracted from them and are loaded under monotonic quasi-static tension up to failure in order to measure the residual strength of 0° plies. Residual tensile strength tests are performed with a 100 kN MTS electromechanical testing machine. As proposed by Payan et al. and De Baere et al. [15,40], a dumbbell shape is used for these specimens (Fig. 8b) in order to keep the failure area away from the specimen tabs and testing machine grips. Specimens are cut by water jet and chamfered $[\pm 45]_{2s}$ glass fibre reinforced composites tabs are stacked at each coupon end.

The accuracy of the axial direction of the $[0/90]_{2s}$ specimen with regard to the longitudinal fibre orientation is also important in order not to turn $[0/90]_{2s}$ coupons into $[\theta/\theta{+}90]_{2s}$ coupons, which would also have consequences for the ultimate tensile strength measurements [38]. This point is investigated hereafter.

2.5. Investigation of the 0° ply misalignment in $[0/90]_{2s}$ extracted specimens

In order to verify that the changes in $[0/90]_{2s}$ specimen residual strength are not related to the misalignment of the 0° plies, a specific investigation was carried out by measuring the longitudinal ply misalignment. A misalignment can be generated by NCF reinforcement material defects, by the lay-up process, by $+45°$ and $-45°$ ply realignment during fatigue loading and by uncertainty over the $[0/90]_{2s}$ specimen extraction process. Hereafter we are interested only in in-plane misalignment because, in contrast to out-of-plane misalignment which is part of material properties, in-plane alignment can be altered by the experimental procedure (lay-up process, testing and extraction).

After specimen extraction, at least one $[0/90]_{2s}$ specimen per $[\pm45]_{2s}$ plate is polished on one edge. Due to the curvature radius of $[0/90]_{2s}$ coupons (Fig. 8b), polishing is only exploitable in tab areas. Once the edge is polished, images are taken with an optical microscope. Image resolution is 1 μm, which gives about 10 pixels in the diameter of one fibre. An example of an image of the whole thickness of the material is provided in Fig. 10. In such images one can see the eight UD plies in the following order [0/90/0/90/90/0/90/0]. Some fibres of 0° plies appear as ellipses in the cut plane, which means that they are not perfectly aligned in the 0° direction.

Ply misalignment at a position is estimated by measuring the mean ellipse along axis L and fibre diameter d (Fig. 10) over at least 50 fibres in the ply, within an observation window of the height of the ply per 1 and 2 mm long. This misalignment $|\theta|$, over a few millimeters, between the tension loading direction and the fibre longitudinal direction is then computed according to the relation:

$$|\theta| = \arcsin\left(\frac{d}{L}\right)$$

The reader's attention must be drawn to the fact that the sign of ply angle of 0° plies cannot be computed with this method. We have only access to the mean absolute value of each fibre angle, which in the case of a ply wavering varying from -1 to $+1°$ would give a mean absolute value not close to 0°. This is due to the fact that the d/L ratio is always positive, while the ply angle is either

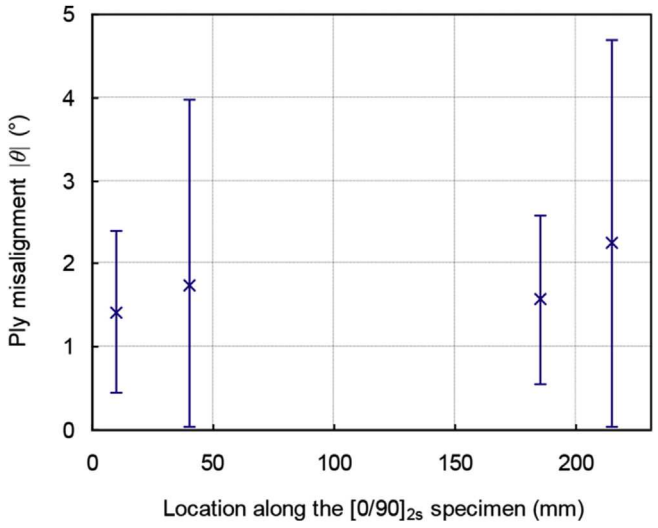

Fig. 11. Misalignment of 0° ply number 1 in a $[0/90]_{2s}$ specimen extracted from a $[\pm45]_{2s}$ specimen with a damage level d_{12} of 0.5.

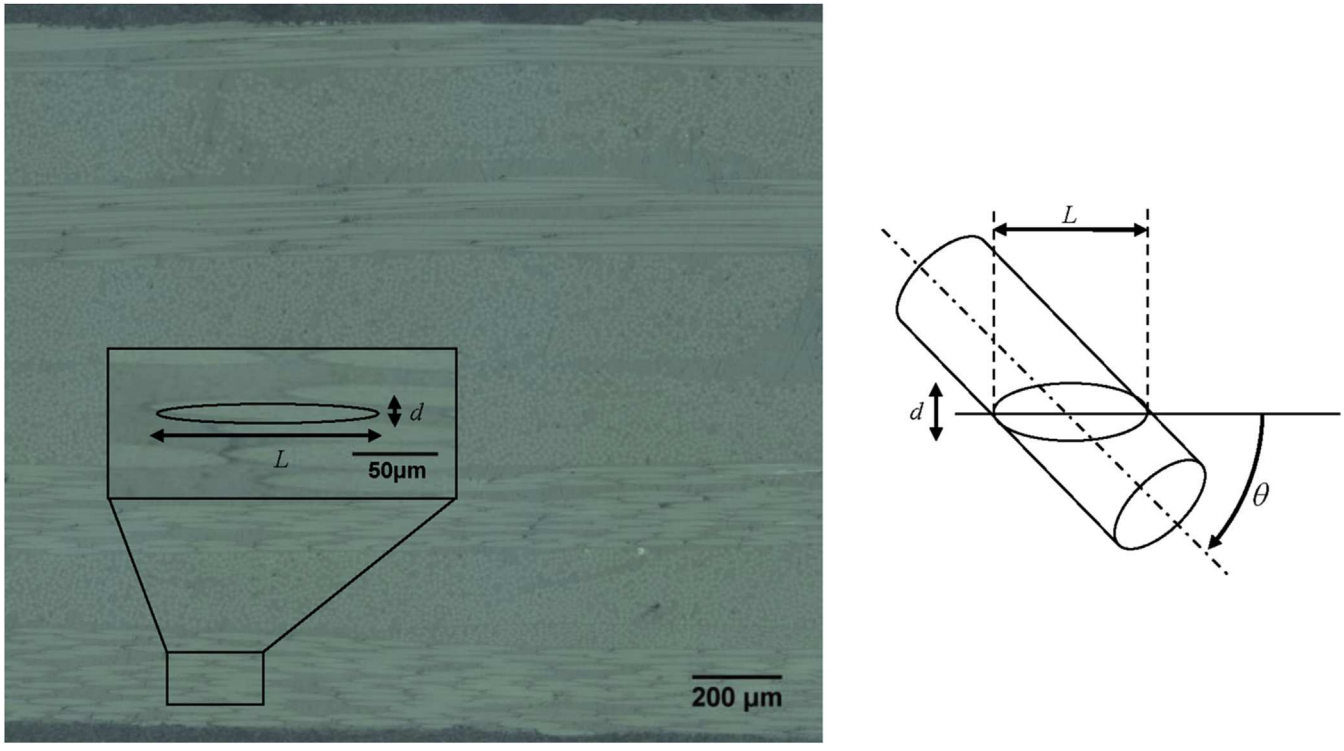

Fig. 10. Investigation of the misalignment of 0° ply of $[0/90]_{2s}$ extracted coupons.

positive or negative. For this reason we would prefer to talk about the misalignment angle rather than the ply angle. This amounts to assuming a global misorientation of the ply but not local undulation.

An example of the results is illustrated in Fig. 11 where the misalignment of the first 0° ply is estimated at four positions along a $[0/90]_{2s}$ specimen extracted from a $[\pm45]_{2s}$ specimen with a damage level d_{12} of 0.5.

On the one hand, these results highlight that the mean misalignment of 0° plies shows a significant scatter either at a single position (within the observation window) or between two separate positions (covering the whole coupon length: 225 mm). The observed scatter, measured as standard deviation, can be more than 3° for the same ply in the coupon length. This deviation can be attributed to the material and the process.

On the other hand, a comparison is possible between the mean misalignment of damaged and undamaged materials. The maximum mean misalignment measured for all plies at all positions of all damaged and undamaged specimens is below 3° and the mean value of all specimens is between 1.5° and 2°. As no significant difference in 0° ply angle was measured between damaged and undamaged specimens, we can therefore consider that possible changes in $[0/90]_{2s}$ specimens' residual strength are not related to 0° ply angle variation.

3. Results

3.1. Residual tensile strength of $[0/90]_{2s}$ specimens

Four large glass-epoxy $[\pm45]_{2s}$ coupons processed by vacuum assisted resin infusion are tested in fatigue under a tension load ratio $R = 0.1$ at a frequency $f = 5$ Hz. Their residual tensile strength and transverse stiffness are obtained as described previously. The residual tensile strength of $[0/90]_{2s}$ specimens is compared to the tensile strength of undamaged material measured on three slender $[0/90]_{2s}$ specimens extracted from a large undamaged $[\pm45]_{2s}$ coupon using the same procedure as for the damaged coupons. As the fibre volume fraction of tested specimens varied from 42% to 49%, results have been adjusted to be compared to the mean fibre volume fraction: $V_f = 46\%$. Test parameters and results are collected in Table 1 and Fig. 12. The different damage levels were obtained by changing the maximum fatigue stress. Fatigue loading was stopped when the target damage level was reached.

A clear decrease in residual tensile strength can be observed when matrix shear damage increases, despite the scatter for each damage level reached. As mentioned in the introduction, this strength loss is assumed to derive from the matrix's loss of capacity to transfer loads between all the fibres when fibre-matrix decohesion and matrix cracks exceed a threshold. The same trend was observed by Hochard et al. for tensile [23] and compressive [41] residual strength on tubes damaged under torsion fatigue loading.

One way to confirm that the decline in strength is linked to matrix function in the composite material is to measure the strength obtained with a test performed at a temperature where the mechanical performances of the matrix become very low [23]. This analysis is detailed in the following section.

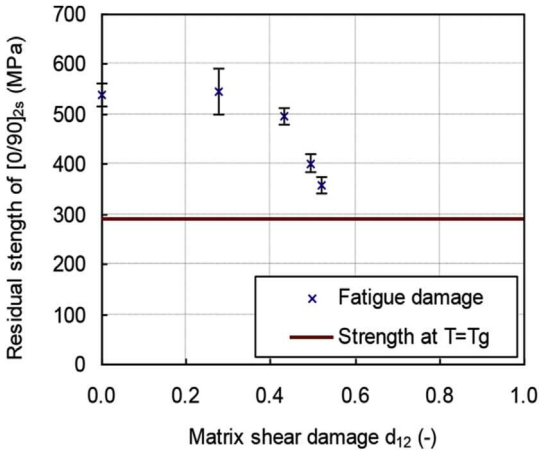

Fig. 12. Residual tensile strength of $[0/90]_{2s}$ specimen as a function of matrix shear damage d_{12} for $V_f = 46\%$.

3.2. Comparison of results with test at 80 °C

An additional monotonic quasi-static tension test was carried out on an undamaged $[0/90]_{2s}$ specimen in a climatic chamber at a controlled temperature of 80 °C. This temperature has been chosen to be equal to the glass transition temperature of the matrix. Running a test at such a temperature should exclude most of the matrix contribution to the mechanical strength of the laminate.

This test revealed a strength decrease of 46% compared to the undamaged material tested at room temperature (20 °C). This strength is shown as a plain red line in the residual strength results in Fig. 12. This test confirms that the matrix plays a large part in fibre direction strength.

It is interesting to note that the tensile strength at 80 °C is close to the tensile strength obtained with the maximal level of matrix damage produced by fatigue loading. This leads us to assume that there is a lower limit of residual strength and that however high the matrix damage, UD ply could always sustain an axial load corresponding to this threshold tensile strength.

3.3. Computation of residual strength of UD ply in fibre direction

In order to use the experimental results on $[0/90]_{2s}$ laminates presented above in a ply scale model, they have to be turned into the residual strength of UD ply in the fibre direction.

At the end of $[0/90]_{2s}$ quasi-static residual strength tests, when the $[0/90]_{2s}$ specimen fails, the 90° plies do not sustain any axial load as it is all carried by 0° plies. This is due to the fact that, as explained in the introduction, when the $[0/90]_{2s}$ laminate reaches a

Table 1
Residual tensile strength and damage parameter d_{12} after cyclic loading under tension $R = 0.1$ for $V_f = 46\%$.

$[\pm45]_{2s}$ specimen ref.	σ_{max} fatigue (MPa)	Number of cycles (−)	d_{12} (−)	Nb. of specimens extracted (−)	Mean residual strength (MPa)	Standard deviation (MPa/MPa)	Residual strength loss (%)
5B	–	0	0	3	537	4.3%	–
8A	57	160 000	0.52	4	359	4.8%	33%
8B	55	65 000	0.50	4	402	4.7%	25%
9A	50	280 000	0.43	4	496	3.6%	8%
9B	40	50 000	0.28	4	546	8.3%	−2%

Table 2
Value of the phenomenological law parameters for $V_f = 46\%$.

Material parameter	Value	Unit
σ_0	1075	MPa
σ_T	576	MPa
d_m	0.49	–
d_λ	0.035	–

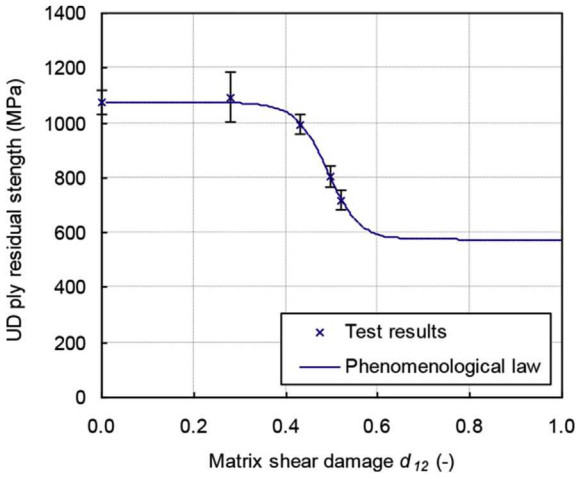

Fig. 13. Residual tensile strength of UD ply in fibre direction as a function of matrix shear damage d_{12} for $V_f = 46\%$, experimental results and phenomenological analytical law.

load that leads to failure, transverse crack density in the 90° plies is so high that these plies cannot carry any load. Axial load is entirely carried by the 0° plies. This phenomenon is true at failure, whatever the matrix damage at the beginning of the quasi-static residual strength test. Therefore, the strength of 0° plies is easily obtained: stress in 0° plies at failure is twice the mean stress sustained by the laminate. Indeed, 0° ply thickness is half of the laminate thickness.

Once the residual strength of UD ply in the fibre direction is computed according to each level of matrix damage, a phenomenological analytical law representing strength versus matrix damage evolution can be proposed. Experimental results highlight two remarkable strength values: σ_0 the reference or initial strength of the UD ply, obtained with specimens not submitted to fatigue damage, and σ_T the bottom threshold, obtained with a tensile strength test at the glass transition temperature. From these two parameters, a law is defined using the following relation to fit experimental data:

$$\sigma_{failure}(d_{12}) = \frac{\sigma_0 - \sigma_T}{1 + e^{(d_{12} - d_m)/d_\lambda}} + \sigma_T \tag{6}$$

In this relation, d_m and d_λ are fitting parameters that describe the damage value of the inflexion point and the shape parameter governing the progressiveness of the law respectively. For the material used in our study, with a fibre volume fraction of 46%, the values identified for these two parameters by a least squares method and the values obtained for σ_0 and σ_T are given in Table 2. The experimental results and the law computed with these parameter values are given in Fig. 13 and show very good agreement.

4. Discussion

The application of the proposed testing procedure to NCF glass-epoxy composite material processed by infusion shows a strong dependency between matrix damage, generated by shear cyclic loading, and residual strength in the fibre direction. This method is very useful to feed fatigue damage models written at the ply scale with meso-scale damage parameters like the one proposed by the LMA-Marseille [23,32]. However, some aspects of the proposed testing procedure, concerning the matrix damage quantification and the influence of the loading mode on the damage mechanisms, require further discussion.

First, the description of the damage at the ply level suggests that the static strength and the fatigue life are driven by the ply behaviour, and that the damage to the interface between the laminate plies can be ignored. Moreover, the proposed quantification of the ply matrix damage is based on in-plane stress state assumption. Observations on the edges of the $[0/90]_{2s}$ specimens, before tensile residual strength tests, showed no macro-delamination, as the reader can see in Fig. 10. Therefore, in-plane stress state assumption seems acceptable for the tests carried out in this study.

Then, the meso-scale parameter chosen to represent the matrix damage (stiffness loss) results from a combination of several damage mechanisms occurring at meso- or micro-scale: fibre-matrix decohesion, transverse cracks, debonding at transverse crack tips (micro-delamination) and matrix plasticity. This combination can differ according to the loading direction (transverse to fibre or shear or combined transverse to fibre and shear). Indeed, shear loading produces mainly diffuse damage at the micro-scale consisting of fibre-matrix decohesion and matrix plasticity, while transverse loading produces more meso-scale damage (transverse crack and micro-delamination at crack tips). Nothing demonstrates that these two types of damage mechanisms give rise to a similar reduction in residual strength in the fibre direction. A more general approach would then consist in defining the residual strength as a function of several damage variables associated to the different damage mechanisms (separating micro-scale phenomena and meso-scale phenomena) as proposed in multi-scale models [13,42]. However, identifying such a function requires completing the proposed experimental procedure with a first test where damage is produced by a transverse loading and a second test where damage is produced by a coupling between transverse and shear loading. The first test could use the same procedure as that proposed in this paper but replacing the [±45] laminate by a [0/90] laminate from where residual strength specimens should be extracted at 90°. For the second test, which aims to generate matrix damage under transverse and shear cyclic loading, the problem is more delicate. Several testing methods could be employed to apply a multi-axial stress state at the ply scale induced by the loading direction: off-axis loaded unidirectional flat specimens, cruciform flat specimens under biaxial loads and thin-walled tubes under combined, tension-torsion, bending/torsion or internal pressure [43]. A multi-axial stress state can also be applied at the ply level, in a laminate with various angles under uniaxial loading, due to the anisotropy of each ply. Among these testing solutions, cruciform flat specimen configuration definition to retrieve exploitable results seems difficult [44] and manufacturing tubes with a representative process of the material found in the structures considered is a not an obvious outcome. The only remaining solution is therefore an off-axis loaded flat UD specimen and laminates under uniaxial loading. Specimen configuration and testing conditions for off-axis tests are non-obvious [22] but these specimens allow large ranges of biaxial ratio of σ_2 to τ_{12}. The second solution proposed is to test a quasi-isotropic laminate, or more generally a laminate with various angles, under uniaxial cyclic loading. In such a laminate, different biaxial ratios of σ_2 to τ_{12} could be observed at the ply level, depending on the proportion of UD plies in each direction but with

much less flexibility than with tubes or off-axis tests. Note also that the evaluation of matrix damage and UD residual strength in such laminates is not direct and would need a dialogue between test results and numerical simulations, including non-linear behaviour.

Finally, it is worth noting that a fatigue life is also observed under purely uniaxial cyclic loading in the fibre direction. This reminds us that residual strength in the fibre direction also depends on cyclic loading in the fibre direction. Two main hypotheses can be put forward to explain this observation. (i) Due to micro-structure effects, cyclic loading in the fibre direction generates a form of matrix damage and consequently a decrease in strength. (ii) Cyclic loading produces fibre damage directly. Further experimental investigations into these phenomena should be carried out in future work.

5. Conclusion and prospects

A testing procedure has been proposed to highlight and characterize UD ply residual strength in fibre direction under quasi-static monotonic tension at 20 °C as a function of its matrix damage, generated by fatigue loading, defined as shear residual stiffness. The advantage of such a method, compared to traditional phenomenological approaches, is to identify a residual strength law a priori independent of the applied load and sequence. Five levels of matrix damage from 0 to 0.5 were produced and results show a strong dependency of the residual tensile strength in fibre direction on matrix damage. An additional quasi-static tension test at the glass transition temperature of the matrix showed that the decrease in fibre tensile strength can reach 46% when the matrix no longer plays a part in the strength of the UD ply.

The law identified with the experimental data obtained in this paper is very useful to feed fatigue damage models written at the ply scale [23,32], and then compute the fatigue life of laminates under cyclic multiaxial loading at the ply scale.

As discussed, complementary work should be carried out, investigating other cyclic loading modes in order to activate other damage mechanisms and their coupling. The use of micro-scale damage parameters in addition to meso-scale parameters to describe the matrix damage is to be considered.

Acknowledgement

Many thanks to Younes Demmouche and more generally to the IRDL team of ENSTA Bretagne where some of the fatigue tests were carried out.

References

[1] Revest N. Comportement en fatigue de pièces épaisses en matériaux composites. PhD thesis. France: École Nationale Supérieure des Mines de Paris; 2011.
[2] Huchette C. Sur la complémentarité des approches expérimentales et numériques pour la modélisation des mécanismes d'endommagement des composites stratifiés. PhD thesis. France: Université Paris 6; 2005.
[3] Talreja R. Stiffness properties of composite laminates with matrix cracking and interior delamination. Eng Fract Mech 1986;25(5–6):751–62.
[4] Stinchcomb WW. Nondestructive evaluation of damage accumulation processes in composite laminates. Compos Sci Technol Jan. 1986;25(2):103–18.
[5] Talreja R. Fatigue of composite materials: damage mechanisms and fatigue-life diagrams. Proc R Soc Lond Ser Math Phys Sci 1981;378(1775):461–75.
[6] Nairn JA. Matrix microcracking in composites. In: Talreja R, Manson J-A, editors. Polymer matrix composites, vol. 2. Elsevier Science; 2000. p. 403–32.
[7] Parvizi A, Garrett KW, Bailey JE. Constrained cracking in glass fibre-reinforced epoxy cross-ply laminates. J Mater. Sci Jan. 1978;13(1):195–201.
[8] Gamstedt EK, Sjögren BA. An experimental investigation of the sequence effect in block amplitude loading of cross-ply composite laminates. Int J Fatigue Feb. 2002;24(2–4):437–46.
[9] Quaresimin M, Carraro PA, Mikkelsen LP, Lucato N, Vivian L, Brøndsted P, et al. Damage evolution under cyclic multiaxial stress state: a comparative analysis between glass/epoxy laminates and tubes. Compos Part B Eng Oct. 2014;61:282–90.
[10] Shen H, Yao W, Qi W, Zong J. Experimental investigation on damage evolution in cross-ply laminates subjected to quasi-static and fatigue loading. Compos Part B Eng Jul. 2017;120:10–26.
[11] Kosmann N, Karsten JM, Schuett M, Schulte K, Fiedler B. Determining the effect of voids in GFRP on the damage behaviour under compression loading using acoustic emission. Compos Part B Eng Mar. 2015;70:184–8.
[12] Ladevèze P, Le Dantec E. Damage modelling of the elementary ply for laminated composites. Compos Sci Technol 1992;43(3):257–67.
[13] Laurin F, Carrere N, Huchette C, Maire J-F. A multiscale hybrid approach for damage and final failure predictions of composite structures. J Compos Mater. Sep. 2013;47(20–21):2713–47.
[14] Krasnobrizha A, Rozycki P, Gornet L, Cosson P. Hysteresis behaviour modelling of woven composite using a collaborative elastoplastic damage model with fractional derivatives. Compos Struct Dec. 2016;158:101–11.
[15] Payan J, Hochard C. Damage modelling of laminated carbon/epoxy composites under static and fatigue loadings. Int J Fatigue Feb. 2002;24(2–4):299–306.
[16] Van Paepegem W, Degrieck J. Modelling damage and permanent strain in fibre-reinforced composites under in-plane fatigue loading. Compos Sci Technol Apr. 2003;63(5):677–94.
[17] Paepegem WV. Fatigue damage modelling of composite materials with the phenomenological residual stiffness approach. In: Vassilopoulos Anastasios P, editor. Fatigue life prediction of composites and composite structures. Woodhead Publishing Limited; 2010. p. 102–38.
[18] Antoniou AE, Kensche C, Philippidis TP. Mechanical behavior of glass/epoxy tubes under combined static loading. Part I: Experimental. Smart Compos Nanocomposites Spec Issue Regul Papaers Oct. 2009;69(13):2241–7.
[19] Lasn K, Echtermeyer AT, Klauson A, Chati F, Décultot D. An experimental study on the effects of matrix cracking to the stiffness of glass/epoxy cross plied laminates. Compos Part B Eng Oct. 2015;80:260–8.
[20] Andersons J, Korsgaard J. Residual strength of GFRP at high-cycle fatigue. Mech Compos Mater. 1999;35(5):395–402.
[21] Rotem A. Residual strength after fatigue loading. Int J Fatigue Jan. 1988;10(1):27–31.
[22] Shokrieh MM, Lessard LB. Multiaxial fatigue behaviour of unidirectional plies based on uniaxial fatigue experiments—II. Experimental evaluation. Int J Fatigue Mar. 1997;19(3):209–17.
[23] Hochard C, Miot S, Thollon Y. Fatigue of laminated composite structures with stress concentrations. Compos Part B Eng Oct. 2014;65:11–6.
[24] Eliopoulos EN, Philippidis TP. A progressive damage simulation algorithm for GFRP composites under cyclic loading. Part I: material constitutive model. Compos Sci Technol Mar. 2011;71(5):742–9.
[25] Eliopoulos EN, Philippidis TP. A progressive damage simulation algorithm for GFRP composites under cyclic loading. Part II: FE implementation and model validation. Compos Sci Technol Mar. 2011;71(5):750–7.
[26] Talreja R. Damage analysis for structural integrity and durability of composite materials. Fatigue Fract Eng Mater. Struct Jul. 2006;29(7):481–506.
[27] Shokrieh MM, Lessard LB. Multiaxial fatigue behaviour of unidirectional plies based on uniaxial fatigue experiments — I. Modelling. Int J Fatigue Mar. 1997;19(3):201–7.
[28] Philippidis TP, Passipoularidis VA. Residual strength after fatigue in composites: theory vs. experiment. Int J Fatigue Dec. 2007;29(12):2104–16.
[29] Post NL, Case SW, Lesko JJ. Modeling the variable amplitude fatigue of composite materials: a review and evaluation of the state of the art for spectrum loading. Int J Fatigue Dec. 2008;30(12):2064–86.
[30] Post NL, Lesko JJ, Case SW. Residual strength fatigue theories for composite materials. In: Vassilopoulos Anastasios P, editor. Fatigue life prediction of composites and composite structures. Woodhead Publishing Limited; 2010. p. 79–101.
[31] Caous D, Bois C, Wahl J-C, Palin-Luc T, Valette J. Analysis of multiaxial cyclic stress state in a wind turbine blade. In: Presented at the 20th international conference on composite materials (ICCM20), copenhagen, Denmark; 2015.
[32] Rakotoarisoa C. Prévision de la durée de vie en fatigue des composites à matrice organique tisses interlock. PhD thesis. France: Université de Technologie de Compiègne; 2014.
[33] Nijssen RPL. Fatigue life prediction and strength degradation of wind turbine rotor blade composites. PhD thesis. Netherlands: Delft University of Technology; 2007.
[34] Brøndsted P, Lilholt H, Lystrup A. Composite materials for wind power turbine blades. Annu Rev Mater. Res 2005;35:505–38.
[35] Stewart R. Wind turbine blade production – new products keep pace as scale increases. Reinf Plast Jan. 2012;56(1):18–25.
[36] Vallons K, Adolphs G, Lucas P, Lomov SV, Verpoest I. Quasi-UD glass fibre NCF composites for wind energy applications: a review of requirements and existing fatigue data for blade materials. Mech Ind 2013;14(3):175–89.
[37] Mandell JF, Samborsky DD. DOE/MSU composite material fatigue database: test methods, materials, and analysis. United States: Sandia National Laboratories; Dec. 1997. Sandia Report SAND97–3002.
[38] Gay D. Matériaux composites. 5ème Edition. Lavoisier; 2005.
[39] Bois C. Mesure et prévision de l'évolution des endommagements dans les composites stratifiés. PhD thesis, Aix-Marseille, France. 2003.
[40] De Baere I, Van Paepegem W, Hochard C, Degrieck J. On the tension–tension fatigue behaviour of a carbon reinforced thermoplastic part II: evaluation of a dumbbell-shaped specimen. Polym Test Sep. 2011;30(6):663–72.
[41] Eyer G, Montagnier O, Hochard C, Charles J-P, Mazerolle F. Effect of damage on

compressive strength in fiber direction for CFRP. In: Presented at the 20th international conference on composite materials (ICCM20), copenhagen, Denmark; 2015.
[42] Ladevèze P, Lubineau G. On a damage mesomodel for laminates: micro–meso relationships, possibilities and limits. Compos Sci Technol Nov. 2001;61(15):2149–58.
[43] Quaresimin M, Carraro PA. On the investigation of the biaxial fatigue behaviour of unidirectional composites. Compos Part B Eng Nov. 2013;54:200–8.
[44] Makris A, Vandenbergh T, Ramault C, Van Hemelrijck D, Lamkanfi E, Van Paepegem W. Shape optimisation of a biaxially loaded cruciform specimen. Polym Test Apr. 2010;29(2):216–23.
[45] Zangenberg J, Brøndsted P, Koefoed M. Design of a fibrous composite preform for wind turbine rotor blades. Mater. Des Apr. 2014;56:635–41.